Available online at www.sciencedirect.com
SCIENCE DIRECT®
ELSEVIER
Nuclear Instruments and Methods in Physics Research B 235 (2005) 309–314
NIM B
Beam Interactions with Materials & Atoms
www.elsevier.com/locate/nimb

Charge exchange and X-ray emission in 70 MeV/u Bi–Au collisions

P. Verma [a,c,d,*], P.H. Mokler [a,b], A. Bräuning-Demian [a], H. Bräuning [b], E. Berdermann [a], S. Chatterjee [a], A. Gumberidze [a], S. Hagmann [e], C. Kozhuharov [a], A. Orsic-Muthig [a], R. Reuschl [e], M. Schöffler [e], U. Spillmann [a], Th. Stöhlker [a], Z. Stachura [f], S. Tashenov [a], M.A. Wahab [c]

[a] *GSI, D-64291 Darmstadt, Germany*
[b] *J. Liebig University, D-35392 Giessen, Germany*
[c] *JMI University, New Delhi 110 025, India*
[d] *Vaish College, Rohtak 124 001, India*
[e] *J.W. Goethe University, D-60486 Frankfurt, Germany*
[f] *Institute for Nuclear Physics, PL-31-342 Cracow, Poland*

Available online 13 May 2005

Abstract

Charge exchange and X-ray emission for 70 MeV/u highly charged ions of Bi^{q+} [$77 \leqslant q \leqslant 82$] colliding with thin Au targets [$21 \leqslant t$ in $\mu g/cm^2 \leqslant 225$] were measured at the heavy ion synchrotron SIS at GSI. For the innermost shells this beam energy implies a quasiadiabatic collision regime. The charge state distribution of the emerging ions was measured by a position sensitive CVD-diamond detector after being analyzed by a magnet spectrometer. Charge exchange cross sections have been deduced from the target thickness dependence of the charge state distribution. Electron capture at distant collision dominates completely over ionization at close collision. The X-ray emission from the collision partners were measured by solid state detectors, Ge(i). The K X-ray emission for closed and open incoming projectile K vacancies gives access to vacancy transfer in the superheavy quasi-molecule transiently formed during collision for the innermost shells.

PACS: 34.70.+e

Keywords: Ion–atom collisions; Charge exchange; K X-ray emission; High Z systems

* Corresponding author. Address: Atomphysik, GSI, Planckstrasse 1, D-64291 Darmstadt, Germany. Tel.: +49 6159 71 2796; fax: +49 6159 71 2701.
E-mail address: P.Verma@gsi.de (P. Verma).

0168-583X/$ - see front matter
doi:10.1016/j.nimb.2005.03.196

1. Introduction

Heavy ion–heavy atom collisions with highly charged projectiles at moderate collision velocities give access to the coupling of the inner-most shells in transiently formed superheavy quasimolecules [1] and hence also to the region of supercritical fields. At the heavy ion synchrotron SIS at GSI, the heaviest ions ($Z\alpha \rightarrow 1$) are available both in the highest charge states (bare, H-like, etc.) and at the same time also at moderate velocities ($v_{ion} < v_k$) [2].

The present study[1] has been undertaken to deduce the charge exchange evolution and charge state cross sections of a relativistic heavy ion penetrating through a very thin solid foil cf. [3] and to correlate the same with X-ray emission cross sections determined for the collision system. The electron/vacancy transfer in inner shells of superheavy quasimolecules is then elucidated. From the charge state evolution, we can to some extent deduce the conditions for quasimolecular collisions inside the solid as a function of penetration depth. Hence, we can extrapolate to vanishing target thickness, i.e. to single collision conditions. In particular we are interested in collisions with an incoming K vacancy of the projectile (Bi^{82+}) which means that we are far off the equilibrium charge state. Here, electron capture in distant collisions dominates completely over ionization in charge exchange. For close collisions and inner shells we are in the adiabatic collision regime. The adiabaticity factor η for the K-shells [$\eta = (v/u)^2$] $\leqslant 0.5$ and the inner shell vacancy transfer can be considered within the quasimolecular picture using diabatic correlation diagrams.

2. Experimental details

A SIS beam of 70 MeV/u Bi^{q+} [$77 \leqslant q \leqslant 82$] was bombarded on thin Au targets of 21, 42, 79, 150 and 225 μg/cm^2 thicknesses (the thinnest ones, 21 and 42 μg/cm^2 targets had ultra thin carbon backings of 11 and 12 μg/cm^2, respectively). The schematic experimental set-up with top view is shown in Fig. 1. The target foils were positioned perpendicular to the beam direction. The projectile and target X-rays emitted were detected by two intrinsic Ge detectors positioned in one plane at 60° forward to the beam direction and by a Si(Li) detector positioned off plane at 45° relative to the two Ge detectors (the latter not shown in the Fig. 1). One of the Ge detectors [7Ge(i)] with dimensions of $25 \times 25 \times 12$ mm^3 was granular with 7 independent stripes of 3.57 mm each (observation angles in the range of 49.2°–70.9° in steps of 3.6°). Whereas the single crystal Ge detector [Ge(i)] with an active area of 500 mm^2 and a crystal thickness of 15 mm had a 4 mm thick Ta collimator with an aperture of 5.8×38 mm^2. Both the detectors had aluminium absorbers in the front to reduce the very high count rate of the L X-rays as compared to the K X-rays of interest. The active solid angles of the 7Ge(i) and Ge(i) detectors were 0.1993sr and 0.0493sr, respectively. The Si(Li) detector (active area 200 mm^2) was used for the detection of the L X-rays.

The ejectiles after being charge state analyzed by a spectrometer were detected by a one-dimensional position-sensitive diamond detector [4,5] (Fig. 1). This newly developed detector (active area of 60×40 mm^2) consists of 32 gold stripes deposited on a polycrystalline chemical vapour deposition (CVD) diamond layer. The stripes are 1.8 mm broad with a 0.2 mm pitch and have an independent read out.

3. Results and discussion

3.1. Charge exchange

Only five primary charge states of the emerging Bi^{q+}-ions could be detected in the focal plane by the position sensitive CVD-diamond particle detector. Thus, the magnetic field of the spectrometer has been shifted after each measurement so as to observe the other lower intensity charge states (Bi^{q-4}, Bi^{q-5}, Bi^{q-6} etc.) keeping an overlap of one charge state for normalization. Fig. 2 shows for example such a "composite charge state distribution" obtained in the particle detector for Bi^{82+}

[1] Part of the Ph.D. thesis work of P. Verma.

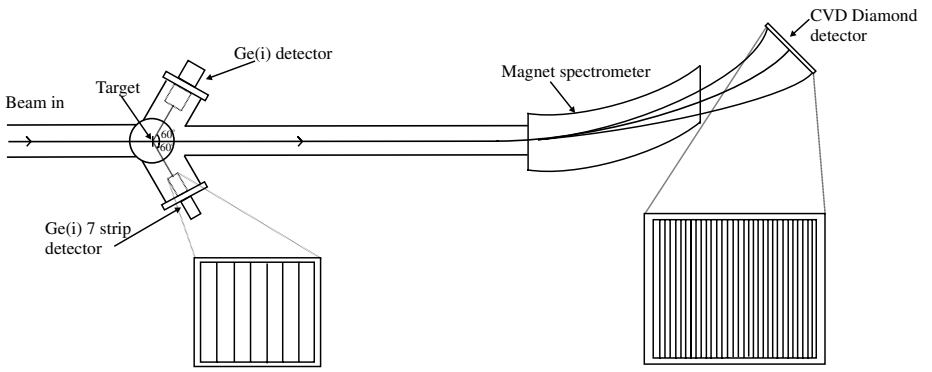

Fig. 1. The experimental set-up showing the Ge X-ray detectors, the magnet spectrometer and the position sensitive CVD-diamond particle detector.

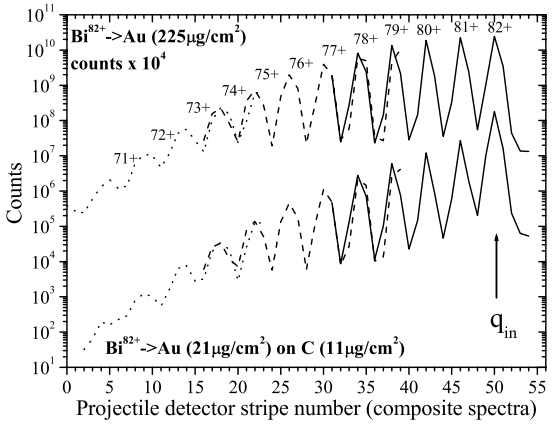

Fig. 2. "Composite charge state distribution" measured by the CVD-diamond position sensitive particle detector for Bi^{82+}-ions incident on Au targets of two extreme thicknesses, 21 and 225 μg/cm^2.

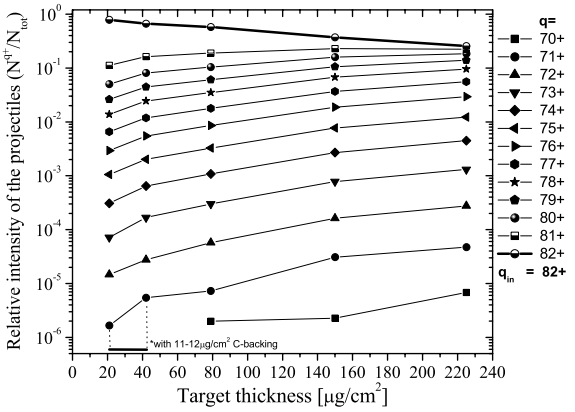

Fig. 3. Charge state fractions (N^{q+}/N_{tot}) of Bi^{82+}-ions as function of Au targets for different thicknesses, N^{q+} refers to the number of projectiles for a particular charge state q+ and N_{tot} to the number of the total projectiles.

-ions incident on Au targets of two extreme thicknesses 21 and 225 μg/cm^2.

The charge state fractions (N^{q+}/N_{tot}) of Bi^{82+}-ions are shown in Fig. 3 as a function of Au target thicknesses (N^{q+} refers to the number of projectiles for a particular charge state q+ and N_{tot} to the number of the total projectiles). In distant collisions, the Bi^{82+}-ions with an incoming projectile K-vacancy capture electrons in the outer shells. From the target thickness dependence of the ratio N^{82+}/N_{tot}, the total electron capture cross section is deduced to be in the order of 3×10^{-18} cm^2. This value is in agreement with the theoretical calculations by the eikonal approach [6] as well as by the semi-empirical non-relativistic scaling formula for NRC [7]. Moreover, the electron capture cross section calculated from the projectile K X-ray emission with incoming K vacancy concurs as discussed below.

3.2. X-ray emission

Fig. 4 shows the K X-ray spectra measured in the laboratory system by the different stripes of the 7Ge(i) detector for Bi^{82+}-ions incident on the thinnest Au target. The target (stationary) X-rays, Au-Kα_2 and Au-Kα_1, stay at the same energy in all the stripes whereas the projectile (moving) X-rays Bi-K$\alpha_{1,2}$ and Bi-K$\beta_{1,2,3,4,5}$, are shifted because of

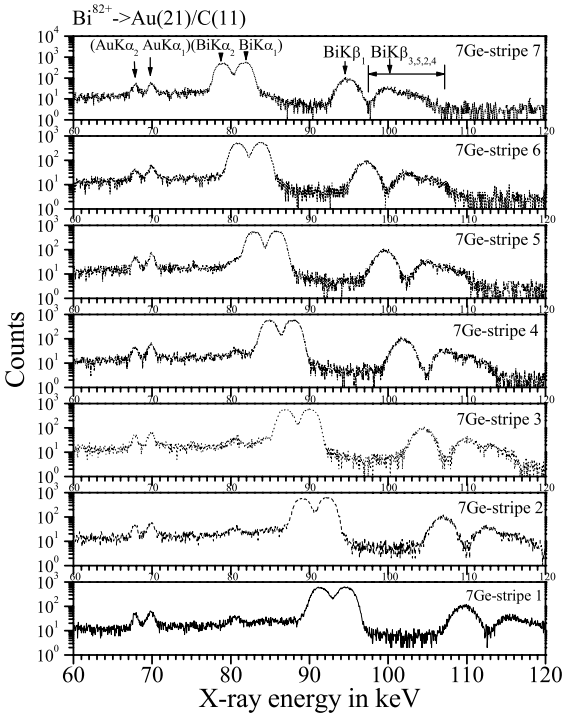

Fig. 4. K X-ray spectra measured in the laboratory frame by the different stripes of the 7Ge(i) detector for Bi^{82+}-ions incident on the 21 μg/cm^2 Au target.

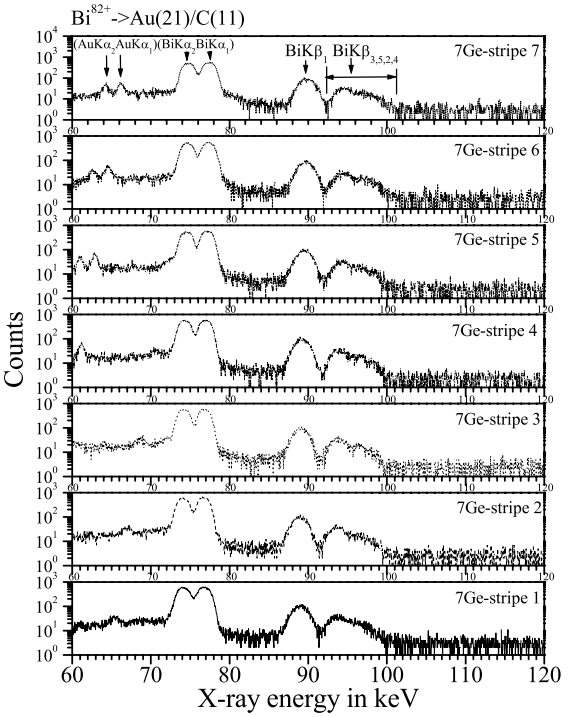

Fig. 5. The spectra shown in Fig. 4 are depicted here after being corrected for Doppler shift.

the angular dependent Doppler shift. For projectiles with an incoming K-vacancy, electron capture by the projectile in its higher shells dominates completely which is followed by subsequent radiative filling of the empty inner shells. Thus the Au-K X-rays have a much smaller intensity as compared to the Bi-K X-rays.

In Fig. 5 these laboratory frame spectra are corrected for Doppler shift. In this representation the projectile K X-rays show same energy in the moving emitter frame and hence coincide for all the stripes. The spectra obtained by the above two methods were added up independently to obtain a total yield for the Au and Bi K X-rays for all the projectile charge state and target thickness combinations investigated. The K X-ray emission cross sections were determined for both the collision partners using the measured detector efficiencies, their solid angles, known target thicknesses as well as the number of normalizing projectile particles measured by the position sensitive diamond detector.

Fig. 6 shows for example $K\alpha_1$ emission cross sections for the projectile Bi and target Au as a function of the incoming charge state (left part) as well as a function of the increasing target thickness

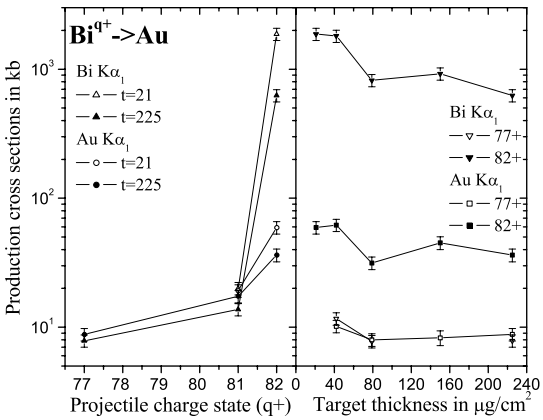

Fig. 6. $K\alpha_1$ emission cross sections for the projectile Bi and target Au as function of the incoming charge state (left part) as well as function of target thickness (right part).

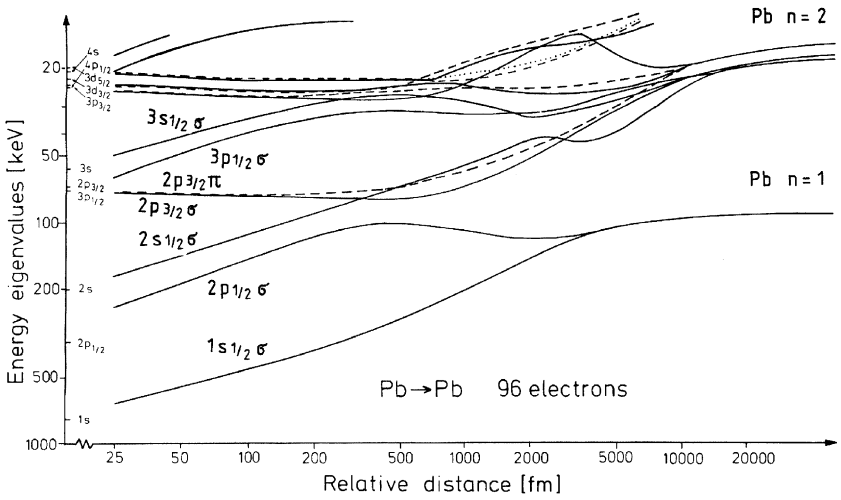

Fig. 7. Diabatic correlation diagram for an equivalent Pb–Pb system according to [8].

(right part). For projectiles having a K vacancy before the collision (Bi^{82+}), the K X-ray emission has been found to increase substantially not only for the projectile (Bi) but also for the target (Au). The increase in the Bi-K emission cross sections indicates a predominance of electron capture from the target to the higher projectile shells and their radiative stabilization, whereas the increase in Au-K emission gives access to the vacancy transfer in the collision molecule. From the increase in Bi-K emission, the collision distance for electron capture can roughly be estimated to be in the order of 12600 fm. Moreover, in close collisions, the K-vacancies for H-like Bi-ions brought into the collision are shared between the projectile and the Au target. From the increase in the Au-K cross sections extrapolated to zero target thickness, the K–K vacancy sharing is deduced to take place around 2300 fm. Fig. 6 also shows clearly that with an incoming K vacancy, the Bi-K and Au-K X-ray cross sections decrease with increasing target thickness which is due to the subsequent filling of the projectile K-vacuum in the solid foil.

4. Conclusion

For interpretation we show in Fig. 7 the diabatic correlation diagram of an equivalent Pb–Pb system [8]. It is clear that the above given estimates of the interaction distance for electron capture and the coupling distance for K–K vacancy sharing conform to the calculated SCF-DFS multielectron level diagram (shown by arrows in Fig. 7). We like to note that the charge states for our collision system are higher than the ones used in calculating the Pb–Pb correlation diagram. So it is not surprising that our estimated coupling distances are somewhat smaller than expected. As is evident from the correlation diagram, the K–K vacancy sharing takes place at a shorter internuclear distance as compared to the electron capture. The capture distance concurs with the region where the atomic levels turn towards molecular ones, i.e. where the corresponding shells start to overlap, whereas the K–K sharing takes place where the quasimolecular $1s\sigma$ and $2p\sigma$ levels start to diverge towards the united atom system.

Acknowledgements

The authors thank B. Franzac of the accelerator group for his kind assistance in getting a very well focussed beam. The active help of the Go4 user's support group, especially J. Adamczewski is gratefully acknowledged for the assistance in the analysis program. P. Verma is indebted to the German Academic Exchange Service (DAAD) for supporting the work as part of the Ph.D. Thesis.

References

[1] P.H. Mokler, D. Liesen, in: Progress in Atomic Spectroscopy, Vol. C, 1984, p. 321.
[2] H.-T. Prinz et al., Hyperfine Interact. 108 (1997) 325.
[3] S. Datz, H.O. Lutz, L.B. Bridwell, C.D. Moak, H.-D. Betz, L.D. Ellsworth, Phys. Rev. A 2 (1970) 430.
[4] E. Berdermann, K. Blasche, P. Moritz, H. Stelzer, B. Voss, Diamond Relat. Mater. 10 (2001) 1770.
[5] P. Moritz, E. Berdermann, K. Blasche, H. Stelzer, B. Voss, Diamond Relat. Mater. 10 (2001) 1765.
[6] A. Ichihara, T. Shirai, J. Eichler, At. Data Nucl. Data Tables 55 (1993) 63;
J. Eichler, Phys. Rev. A 32 (1985) 112.
[7] A.S. Schlachter, J.W. Stearns, W.G. Graham, K.H. Berkner, R.V. Pyle, J.A. Tanis, Phys. Rev. A 27 (1983) 3372.
[8] M. Mann, P.H. Mokler, B. Fricke, W.-D. Sepp, W.A. Schonfeldt, H. Hartung, J. Phys. B 15 (1982) 4199.